

1

Supporting information

2

3

Performance and characteristics of fluoride adsorption using

4

nanomagnetite graphite-La adsorbent

5

6

Shuangxi Wen, Yili Wang*, Shuoxun Dong

7

Beijing Forestry University, Beijing 100083, China

8

9

***Corresponding author:** Yili Wang; Phone: +86-10-62336673; Fax: +86-10-

10 62336596; E-mail: wangyilimail@126.com

11

12

*Corresponding author. Tel.: +86 10 62336673; fax: +86 10 62336596.
E-mail address: wangyilimail@126.com (Y.L. Wang).

13 1 SEM images and EDX detection

14 The surface morphology of NG, MGNP, MGLNP and MGLNP loaded with fluoride
15 was shown in Fig. S1. Fig. S1b indicated that lots of nano-Fe₃O₄ particles were
16 successful loaded on the NG. In Fig. S1c, the brighter regions correspond to the
17 lanthanum particles,¹ that was confirmed by EDS analysis (Fig. S2).

18

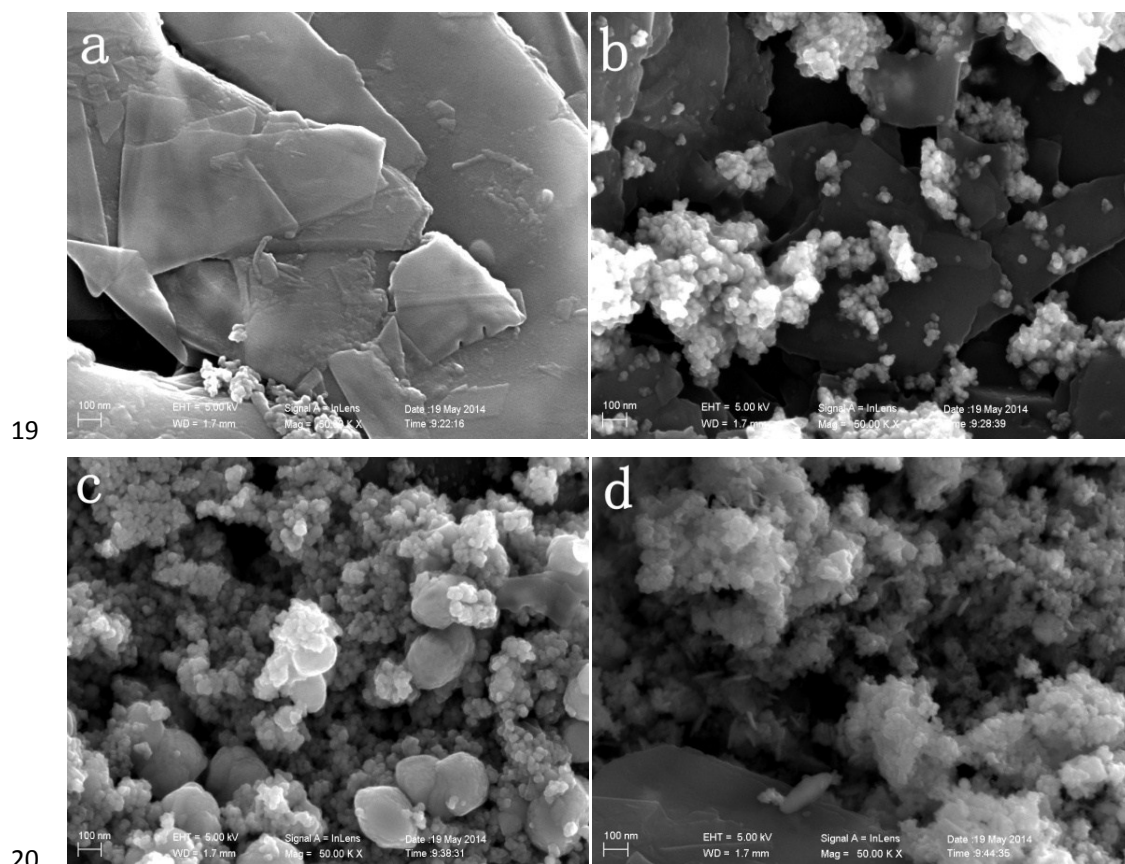


Fig. S1. SEM micrographs: (a) NG; (b) MGNP; (c) MGLNP and (d) F⁻ loaded MGLNP.

Fig. S2c showed that the γ -Fe₂O₃ and La ions are successfully immobilized on the surface of adsorbent.

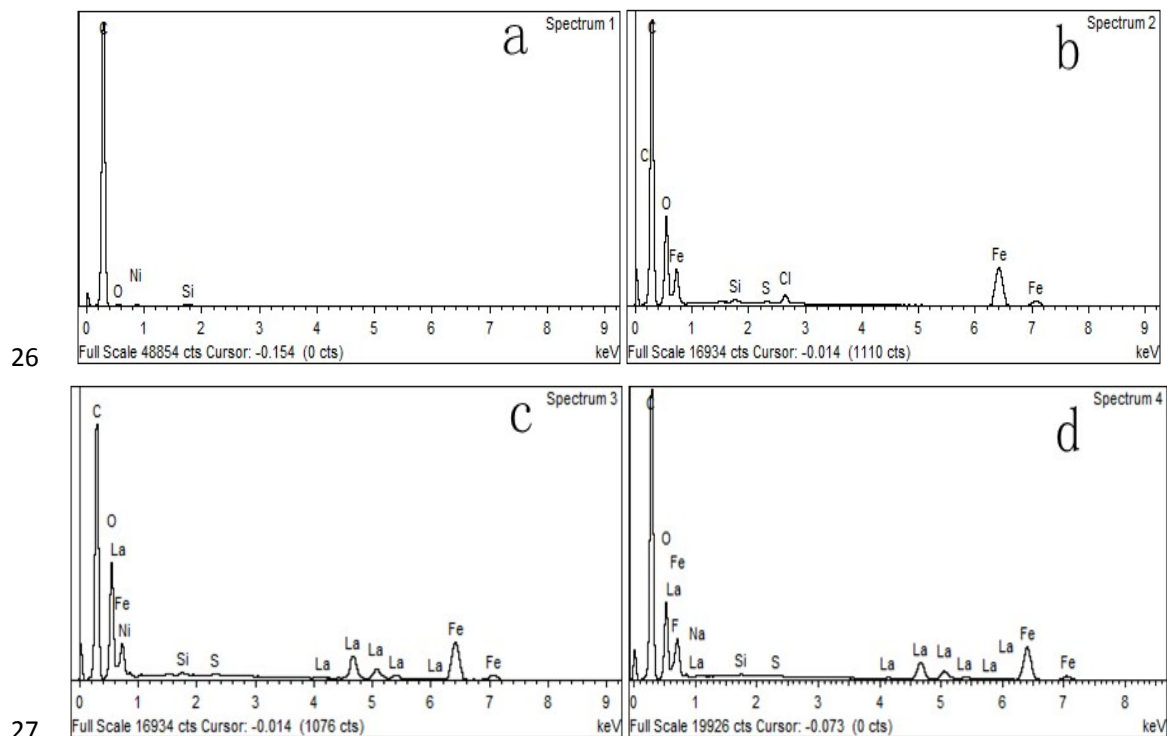
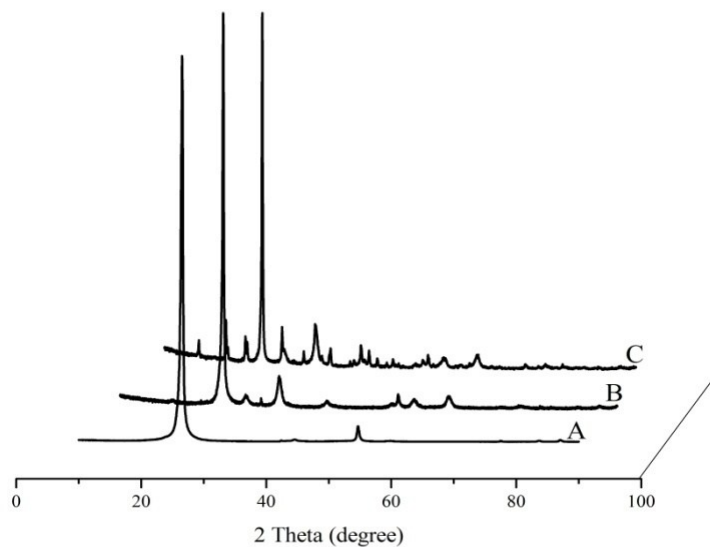


Fig. S2. EDX images: (a) NG; (b) MGNP; (c) MGLNP and (d) F⁻ loaded MGLNP.

31 2 XRD patterns

32 X-ray diffraction patterns of all the samples were investigated by a X-ray
 33 diffractometer, Model D8, BRUKER AXS, using Cu K α radiation ($\alpha = 0.15425$ nm)
 34 in the range of 2θ from 10° to 90° . The results are displayed in Fig. S3. In Fig. S3(A),
 35 the typical peak of nano-graphite (NG) was identified at $2\theta = 26.5^\circ$. In Fig. S3(B), the
 36 typical peaks of Fe₃O₄ at $2\theta = 30.2^\circ, 35.6^\circ, 43.2^\circ, 57.5^\circ$ and 62.7° indicated that the
 37 nano-Fe₃O₄ particles were loaded on the surface of NG. After the MGNP was
 38 immersed by saturated La(NO₃)₃·6H₂O solution and calcined at 300 °C for 3 h, the
 39 nano-Fe₃O₄ particles were transformed into γ -Fe₂O₃, Fig. S3(C) shows the X-ray
 40 diffraction of γ -Fe₂O₃-graphite-La (MGLNP), which includes all the peaks of graphite,
 41 γ -Fe₂O₃ and La ($2\theta = 30.1^\circ, 38.2^\circ, 44.8^\circ, 49.8^\circ, 54.7^\circ$ and 57.4°).²



42

43

Fig. S3. XRD patterns: (A) NG; (B) MGNP and (C) MGLNP.

44

45 **3 Cost analysis**

46 On the basis of market investigation, the cost of MGLNP preparation was determined

47 as following:

48

Tab. S1. Cost analysis of MGLNP adsorbent.

Item	Price	Dose per Kg MGLNP	Cost (US \$·kg ⁻¹ MGLNP)	Total price (US \$·kg ⁻¹ MGLNP)
Nanographite powder	76.92 US \$·kg ⁻¹	0.43 kg	33.08	
FeCl ₂ ·4H ₂ O	1.38 US \$·kg ⁻¹	0.17 kg	0.24	
FeCl ₃ ·6H ₂ O	0.71 US \$·kg ⁻¹	0.45 kg	0.32	
Ammonia	0.69 US \$·kg ⁻¹	0.98 kg	0.69	
La(NO ₃) ₃ ·6H ₂ O	53.85 US \$·kg ⁻¹	0.78 kg	42.00	79.71
Concentrated nitric acid	2.46 US \$·L ⁻¹	0.58 L	1.40	
Concentrated sulfuric acid	1.08 US \$·L ⁻¹	0.98 L	1.06	
Water	0.77 US \$·t ⁻¹	0.15 t	0.12	
Electricity	0.10 US \$·kW ⁻¹	8 kW	0.80	

49 The cost of MGLNP could be divided into several items: materials and reagents,
 50 water and electricity. In total, the price for MGLNP adsorbent is 79.71 US \$·kg⁻¹,
 51 which is higher than some low-cost adsorbents derived from either natural or waste
 52 sources as show in Tab. S2.³ However, MGLNP adsorbent had high adsorption
 53 capacity of 77.12 mg·g⁻¹ at 25 °C, and even remained higher than 75% adsorption
 54 capacity after three cycles of fluoride adsorption. Therefore, MGLNP adsorbent had a
 55 potential for fluoride removal from drinking water.

56 **Tab. S2.** Comparison between various adsorbents used for fluoride removal on
 57 the basis of adsorption capacity and cost of used material.

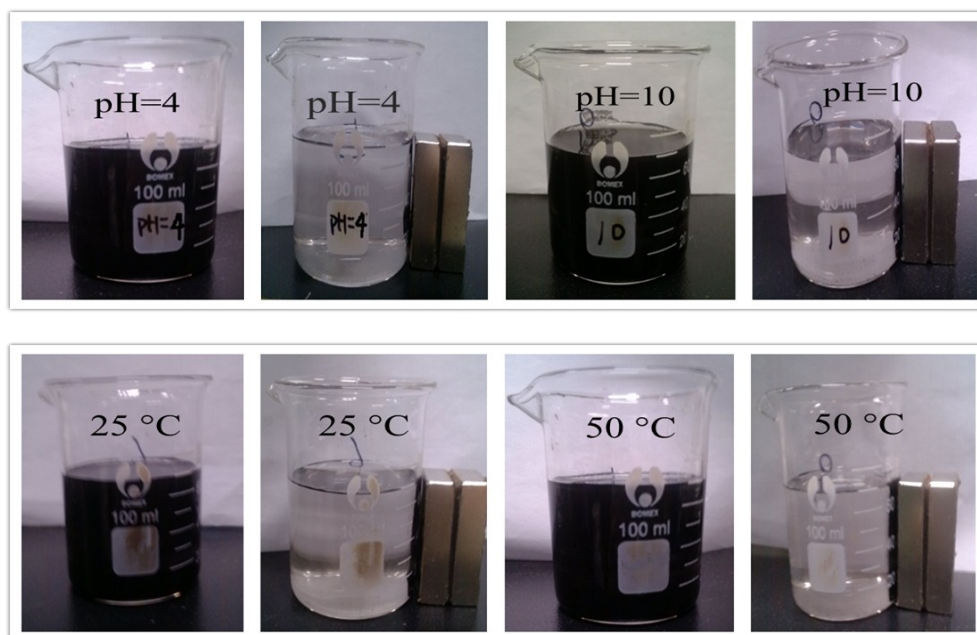
Adsorbent	Adsorption capacity (mg·g⁻¹)	Estimated cost (US \$·kg⁻¹)
Activated alumina	2.40	~2.30
Amorphous alumina	3.60	~70.00
Activated carbon (ALC-300)	1.10	~25.00
Calcite	4.37×10 ⁻⁵	~0.11
Clay (bentonite)	7.09	~1.00
Charcoal	7.88×10 ⁻⁵	~0.32
Red mud	6.28×10 ⁻³	~0.10
Carbon slurry	4.86	~0.20
MGLNP	77.12	~79.71

58 **4 Stability of the MGLNP**

59 The effects of temperature (25°C, 35°C and 50°C) and pH (4~10) on magnetic
 60 separation and equilibrium adsorption capacity have been studied. The corresponding
 61 experiments were conducted as below:

62 Firstly, several 100 ml MGLNP suspensions of 10 g·L⁻¹ in the polyethylene
 63 bottles were shaken for 8 days at 160 rpm in the air bath thermostat oscillator.

64 Afterward, the MGLNP in the suspensions was separated under a magnetic field. Fig.
65 S4 presented the magnetic separation results accordingly. As treated with different pH
66 values or temperatures, the MGLNP could be easily separated with magnet, and the
67 black opaque suspension rapidly changed to clear liquid.



68

69

70 **Fig. S4.** Magnetic separation of treated MGLNP with different pH values or
71 temperatures.

72 Subsequently, the magnetically separated MGLNP was dried at 60 °C for 8h.
73 The fluoride adsorption experiments with these dried MGLNPs were carried out
74 according to the procedure in section 2.3 of the manuscript. 20 mg MGLNP adsorbent
75 was dosed into 100 ml F⁻ solution with the concentration of 9.88 mg·L⁻¹, then this
76 suspension was shaken at 160 rpm and 25 °C in the air bath thermostat oscillator. Tab.
77 S3 showed the corresponding equilibrium adsorption capacities (Q_e).
78

80 **Tab. S3.** Equilibrium adsorption capacities of treated MGLNP with different pH
81 values or temperatures.

Q_e for original MGLNP ($\text{mg}\cdot\text{g}^{-1}$)	Q_e for 8-day treated MGLNP ($\text{mg}\cdot\text{g}^{-1}$)									
	pH = 4.0	pH = 5.0	pH = 6.0	pH = 7.0	pH = 8.0	pH = 9.0	pH = 10.0	t = 25 °C	t = 35 °C	t = 50 °C
18.10	14.13	16.63	17.27	17.80	17.63	17.77	17.93	18.03	17.97	17.27

82 As indicated in Tab. S3, most Q_e values of 8-day treated MGLNPs showed slight
83 difference except for the 8-day treated MGLNP with pH = 4.0, which decreased from
84 18.10 $\text{mg}\cdot\text{g}^{-1}$ of the original MGLNP to 14.13 $\text{mg}\cdot\text{g}^{-1}$.

85 5 The quantitative analysis of the adsorption mechanism

86 In order to further analysis of defluorination mechanism, the fluoride removal data
87 were estimated through quantitatively calculating the $[\text{OH}^-]$ increase and the loaded
88 La^{3+} on the surface of MGLNP. The corresponding result is shown in Tab.3. The
89 quantitative analysis of the adsorption mechanism is provided as following:

90 **Tab. S4.** The quantitative analysis of the adsorption mechanism (adsorbent dosage =
91 200 $\text{mg}\cdot\text{L}^{-1}$, 25 °C).

Mechanism	Before adsorption	After adsorption	Difference	Adsorption capacity ($\text{mg}\cdot\text{g}^{-1}$)
F^- ion exchange with OH^-	pH = 6.94	pH = 8.98	$\Delta[\text{F}^-] = \Delta[\text{OH}^-] =$ 0.18 $\text{mg}\cdot\text{L}^{-1}$	0.90
Surface La^{3+} complexation with F^-	Loaded $\text{La}^{3+} = 254.26$ $\text{mg}\cdot\text{g}^{-1}$	Adsorbed $\text{F}^- =$ 104.31 $\text{mg}\cdot\text{g}^{-1}$	$q = 104.31 \text{ mg}\cdot\text{g}^{-1}$	104.31

92 As indicated in Tab. 3, the calculated F^- adsorption capacity of MGLNP is
93 105.21 $\text{mg}\cdot\text{g}^{-1}$, which is higher than the maximal adsorption capacity (Q_m) for fluoride
94 determined with the Langmuir model were 77.12 $\text{mg}\cdot\text{g}^{-1}$ at 25 °C. This difference
95 could be attributed to a part of La^{3+} loading on the MGLNP without F^- complexation.

96 Therefore, the calculated adsorption capacity of $104.31\text{mg}\cdot\text{g}^{-1}$ was overestimated, and
97 surface La^{3+} complexation mechanism played an important role in the fluoride
98 removal by MGLNP.

99 **Reference**

- 100 1 L. Gao and L.G. Chen, *Microchim Acta*, 2013, 180, 423–430.
- 101 2 E. Vences-Alvarez, L.H. Velazquez-Jimenez, L.F. Chazaro-Ruiz, P.E. Diaz-Flores
102 and J.R. Rangel-Mendez, *J Colloid Interface Sci*, 2015, 455, 194-202.
- 103 3 S. Jagtap, M.K. Yenkie, S. Das and S. Rayalu, *Desalination*, 2011, 273, 267-275.

104

105